Mathematical Biosciences and Engineering

MBE, 19(4): 3909–3927.
DOI: 10.3934/mbe.2022180
Received: 28 December 2021
Revised: 25 January 2022
Accepted: 07 February 2022
Published: 11 February 2022

http://www.aimspress.com/journal/MBE

Research article

A novel compact broadband and radiation efficient antenna design for medical IoT healthcare system

Zaheer Ahmed Dayo[1,*], Muhammad Aamir[1,*], Shoaib Ahmed Dayo[2], Imran A. Khoso[3], Permanand Soothar[4], Fahad Sahito[5], Tao Zheng[6], Zhihua Hu[1,*] and Yurong Guan[1]

[1] College of Computer Science, Huanggang Normal University, Huangzhou 438000, China
[2] Department of Industrial Engineering, Universita Degli Studi Di Salerno (University of Salerno)-Via Giovanni Paolo II, Fisciano (SA) 132-84084, Italy
[3] College of Electronic and Information Engineering, Nanjing University of Aeronautics and Astronautics, China
[4] School of Electronic and Optical Engineering, Nanjing University of Science and Technology, Nanjing 210094, China
[5] College of Electronic and Communication Engineering, Beijing University of Posts and Telecommunication, Beijing 100879, China
[6] Deputy General Manager, Nanjing Hurys Intelligent Technology Company Limited, Nanjing, China

* **Correspondence:** Email: zaheerdayo@hgnu.edu.cn, dayo.zaheer@hotmail.com, aamirshaikh86@hotmail.com, huzhihua@hgnu.edu.cn.

Abstract: This paper investigates and develops a novel compact broadband and radiation efficient antenna design for the medical internet of things (M-IoT) healthcare system. The proposed antenna comprises of an umbrella-shaped metallic ground plane (UsMGP) and an improved radiator. A hybrid approach is employed to obtain the optimal results of antenna. The proposed solution is primarily based on the utilization of etching slots and a loaded stub on the ground plane and rectangular patch. The antenna consists of a simple rectangular patch, a 50 Ω microstrip feed line, and a portion of the ground plane printed on a relatively inexpensive flame retardant material (FR4) thick substrate with an overall compact dimension of 22 × 28 × 1.5 mm^3. The proposed antenna offers compact, broadband and radiation efficient features. The antenna is carefully designed by employing the approximate calculation formulae extracted from the transmission line model. Besides, the parameters study of important variables involved in the antenna design and its influence on impedance matching performance are analyzed. The antenna shows high performance, including

impedance bandwidth of 7.76 GHz with a range of 3.65–11.41 GHz results in 103% wider relative bandwidth at 10 dB return loss, 82% optimal radiation efficiency in the operating band, reasonable gain performance, stable monopole-shaped radiation patterns and strong current distribution across the antenna lattice. The suggested antenna is manufactured, and simulation experiments evaluate its performance. The findings indicate that the antenna is well suited for medical IoT healthcare systems applications.

Keywords: compact; broadband; radiation efficiency; umbrella-shaped metallic ground plane (UsMGP); modified radiator and medical internet of things (M-IoT) healthcare systems

1. Introduction

The great progress of wireless medical healthcare systems needs compact broadband and efficient antennas. The optimal performance of these systems is achieved with the robust antenna designs. Recently, compact antenna devices have been playing an important role. These devices are part of the modern healthcare wireless communication system. Therefore, designing a compact antenna with the best performance is still a challenging task for active antenna designers. In addition, different types of antennas with different specifications covers modern heterogeneous wireless applications have been reported in the literature [1–4]. The existing antenna designs still faces many challenges, such as reasonable antenna behaviour, narrow bandwidth (BW), moderate radiation efficiency and acceptable gain with the comparatively larger size.

In recent years, there has been remarkable research and advancement in the medical internet of things (M-IoT) and healthcare systems and services [5,6]. The M-IoT has proved its ability to connect disparate pieces of medical equipment, sensors, actuators, and healthcare professionals to provide superior medical services at a remote location [7–10]. As a result, many benefits have been achieved, including optimized patient safety, lower healthcare costs, increased healthcare service accessibility and increased operational efficiency in M-IoT field [11,12]. The M-IoT technology encompasses heterogeneous wireless communication applications (HWCA) used in smart gadgets, control and automation systems, wireless sensor networks and smart grids [13,14]. A significant role is played by the efficient antenna system utilized in M-IoT end devices. An M-IoT system uses an efficient antenna design with features including compact, low-cost, broadband, low power consumption, radiation efficiency, simple configuration, and monopole-like radiation patterns.

Moreover, researchers are drawn to a high-performance broadband system due to its fast data rate, high capacity, simplicity, and low operational power. Nowadays, scholars concentrate their efforts on developing antennas with novel structures and increased compact properties. The antennas may utilize the entire spectrum without causing interference in a confined space. These antennas are distinguished by their broad bandwidth, high gain, small size, and great radiation efficiency. The antennas can be used to cover M-IoT, modern heterogeneous wireless communication applications (HWCA), including civil and military wireless access services, personal communication system, airborne, naval, terrestrial radio detection and ranging (RADAR) [15], high-speed modern M-IoT [16], high-precision positioning satellite and navigational systems and so on. The telecommunication regulatory authority radio frequency allocation board of the Federal Communication Commission (FCC) has apportioned spectrum for multiple HWCA, such as C-band from 4 to 8 GHz, X-band from

8 to 12 GHz, H-band from 6 to 8 GHz [17], and airborne, terrestrial and naval radars from 8.5 to 10.5 GHz, respectively.

References [18–21] have been made to current research on miniature high-performance planar antennas for modern wireless communication applications. Diverse radiator shapes and modern antenna topologies, including folded C-shaped radiator and disc-shaped antenna for radio frequency identification and broadband applications reported in [22,23]. In references [24–26], an elliptical wide-slot antenna with a cross-shaped parasitic component, redesigned antenna lattices utilizing defected ground structures (DGS), and meta-material resonator inspired antennas for ultra-wideband (UWB) applications were presented. A compact circular staked patch antenna achieved a wide BW of 5.02 GHz [27]. Another hexagonal probe-fed antenna using a flangeless connector exhibited 8.3 GHz BW with a reasonable gain performance developed in [28]. The authors used various antenna shapes to achieve a broad impedance BW and did not emphasize the radiation efficiency. A miniature trident antenna by engraving multi-resonant slots and annular sector for UWB applications were presented in [29]. The broadband antenna with loading u-shaped patch engraved on the compact substrate 40 × 50 × 1.575 mm^3; achieved around 40% fractional BW have been designed in [30]. Another work presented the high-performance Fabry-Perot cavity antenna using a beam switched approach. The designed antenna attained the 24% relative BW and 17.6 dBi peak realized gain at a given frequency range [31]. However, the developed antennas include intricate topologies and higher antenna diameters. Roberto Vincenti Gatti et al. designed the single layer wideband antenna using a microstrip feeding line. The authors utilized the square and rectangular patches with compact sizes of 9.85 × 9.85 mm^2 and 9.403 × 11.593 mm^2. The presented work achieved a reasonable BW of 6.12% and 3.17% in the operating band [32]. The stubs loaded patch DGS, and numerous designing concepts of broadband antennas were utilized in [33,34]. A dual wideband antenna with parasitic slot and radiator was reported in [35]. The proposed antenna achieved 2.4 to 6.1 GHz and 9.4 to 13.8 GHz impedance BW. The method for BW enhancement has been suggested in [36]. The authors achieved the broad BW with compact fractal metal structures. A wideband antenna with notch band features and improved patch antenna design were suggested in [37,38]. However, the employed approaches were complex, resulting in computational complexity. A miniaturized broadband patch and slot antennas for ground penetrating radar (GPR) and multiple-input multiple-output (MIMO) wireless terminal applications were reported in [39,40]. The antennas enhanced results were achieved with larger substrate dimensions.

Further, a new palm tree structure antenna with wideband features proposed in [41]. The antenna achieved the broadband BW ranging from 4.0–10.4 GHz. The triple band notch wideband panda-shaped antenna exhibited reasonable results across the frequency span was demonstrated in [42]. Recently, UWB, single and dual resonant antennas for spectrum sensing and moisture content measurement applications reported in [16,43]. The compact antennas with asymmetric coplanar strip (ACS) feeding and coplanar waveguide (CPW) feeding approaches were reported in [44–46]. The designed antennas achieved the triple and pentaband features by using the material selection and different shaped slots. The authors have used different laminates to achieve good performance of the antennas. Another new design of antenna fed with CPW feed line achieved reasonable gain performance and 67% efficiency for satellite forward mission features proposed in [47]. The designed antenna has the overall size of 40 × 40 mm^2 imprinted on Roggers 5880 laminate. Further, the reconfigurable and versatile designing methods for single and multiple elements were analyzed in [48–50]. An ultra-compact triangular-shaped ground plane antenna have been proposed for

multiband features [51]. Besides, a broadband antenna for modern communication application reported in [52]. The antenna with an inverted omega-shaped ground plane achieved wideband and high gain features reported in [53]. A miniaturized crossed dipole antenna with a size of 30.3 × 51.4 × 0.508 mm^3 achieved the 28% fractional BW, and 1 × 8 dielectric resonator antenna (DRA) array exhibited an optimal gain of 12 dBi and BW of 6 GHz were reported in [54,55]. The employed antenna designing methods were complex and time-consuming. The antenna's high-performance results including good impedance BW and high gain demonstrated in [15,56]. The results were accomplished using an array and a single layer stub loaded approaches. The slotted bowtie elements transmit array for UWB applications was proposed in [57]. The authors designed different antenna geometries with multiple functionalities for different modern communication applications reported in [58,59]. The other studies about the high-performance dipole antennas using cavity backed approach and modified taegeuk structure were reported in [60–62].

This article proposes a revolutionary compact broadband and radiation efficient antenna with an umbrella-shaped metallic ground plane (UsMGP). A new hybrid approach is employed to obtain the optimal antenna results. The primary reason for this compact antenna design is to introduce a novel structure that may achieve wide impedance bandwidth (BW), optimal radiation efficiency and stable omni-directional radiation patterns. The proposed method mainly relies on etching slots and loaded stub used on the ground plane and rectangular patch. The proposed antenna includes a simple rectangular patch, 50 Ω microstrip feed line, and ground plane. The antenna design is printed on a thick layer of low-cost flame retardant (FR4) substrate material. The antenna is designed to be compact with an overall size of 22 × 28 × 1.5 mm^3. The parameters study of important variables involved in the antenna design and its influence on impedance matching performance are analyzed. The proposed antenna model obtains an impedance bandwidth of 7.76 GHz with a range of 3.65–11.41 GHz results in a wider fractional BW of 103%, a reasonable gain of 4.58 dBi, stable monopole like radiation pattern and good 82% radiation efficiency features. The suggested antenna design has been simulated, constructed, and verified experimentally. As demonstrated by simulation and experimental findings, the suggested compact broadband and radiation efficient antenna is a superior solution for M-IoT healthcare systems.

The remainder of the manuscript is organized as follows. Sections 2 and 3 describe the proposed antenna's technological plan and evolution stages. Section 4 comprises the simulation results and discussion; Section 5 includes experimentally validated results; Section 6 contains a comparison to recently published state-of-the-artwork. Finally, Section 7 summarizes the concluding observations.

2. Antenna technical design strategy

In this section, the proposed antenna technical design strategy is briefly described. Before start designing the antenna lattice, the type of antenna, selection of the material and its thickness is very important. Based on the requirement, the planar monopole antenna (PMA) has been focused due to its good performance and low-cost FR4 epoxy substrate material is used to curb the fabrication cost of the antenna. Afterwards, selection of suitable electromagnetic (EM) software has been decided. The antenna is designed and simulated by using the high frequency structure simulator (HFSS) version 13.0. The step by step flow of technical strategical plan of the proposed antenna is briefly explained. The proposed antenna is designed by employing the transmission line model equations. The antenna is designed using the following technical approach illustrated in Figure 1.

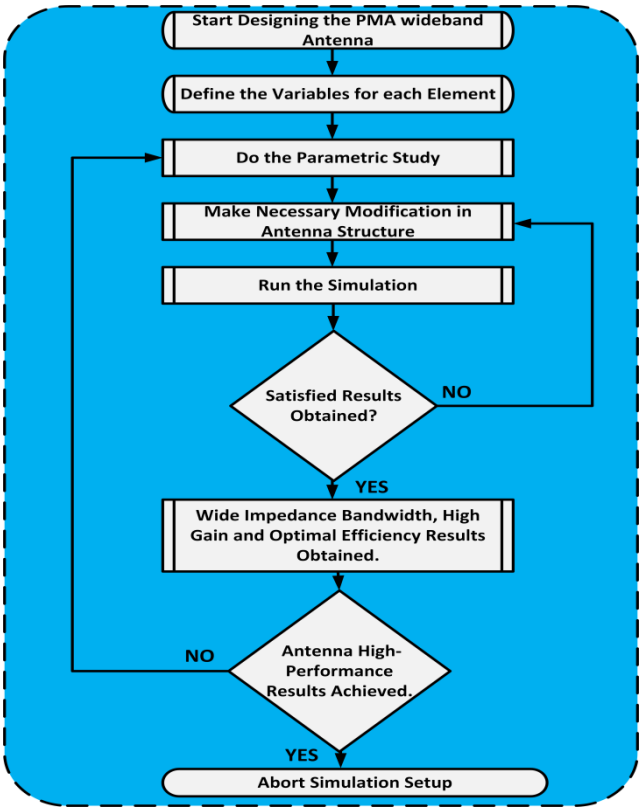

Figure 1. Flow chart of designed technical strategy.

Besides, the approximated mathematical formulation based on the transmission line model is also expressed here. The size of the radiating patch, dielectric substrate, feed line and partial ground plane of the proposed antenna can be obtained by the following approximated Eqs (1) to (9). The value of patch length can be obtained by using the formula [52]:

$$LoP = L_{eff} - 2 \times \Delta L \tag{1}$$

where, LoP represents the patch length, L_{eff} is the effective length, and ΔL is the normalized extension in length. Moreover, L_{eff} can be calculated as follow:

$$L_{eff} = \frac{V_0}{2f\sqrt{\varepsilon_{reff}}} \tag{2}$$

where, V_0 denotes the speed of light in a vacuum, f represents the resonance frequency, and ε_{reff} indicates the effective dielectric constant. Furthermore, ε_{reff} can be calculated as follow:

$$\varepsilon_{reff} = \frac{\varepsilon_{reff}+1}{2} + \frac{\varepsilon_r - 1}{2\sqrt{1+12\left(\frac{HoS}{WoS}\right)}} \tag{3}$$

where, ε_r is the dielectric constant of the substrate, HoS and WoS, represents the dielectric substrate's height and width, respectively. Moreover, normalized extension in length due to the fringing effect can be calculated as follows:

$$\Delta L = 0.412 \times HoS \left[\frac{\left(\varepsilon_{reff} + 1\right)\left(\frac{WoP}{HoS} + 0.264\right)}{\varepsilon_{reff} - 0.258\left(\frac{WoP}{HoS} + 0.8\right)} \right] \tag{4}$$

where, *WoP* represents the width of the patch. Moreover, the width of the patch (*WoP*) and length of the partial ground plane (*LoGP*) can be calculated as follow:

$$WoP = \frac{V_0}{2f}\left[\sqrt{\frac{2}{\varepsilon_{reff} + 1}}\right] \tag{5}$$

$$LoGP = LoP + 6 \times HoS \tag{6}$$

where, *LoP* is the length of the patch. However, substrate thickness (*HoS*), width of the ground plane (*WoGP*), feed line length (*LoF*) and guided wavelength (λ_g) can be calculated as follow:

$$HoS = \frac{0.606 \times \lambda}{\sqrt{\varepsilon_r}} \tag{7}$$

$$WoGP = WoP + 6 \times HoS \tag{8}$$

$$LoF = \frac{\lambda_g}{4}; \lambda_g = \frac{\lambda}{\sqrt{\varepsilon_{reff}}} \tag{9}$$

3. Antenna evolution stages and designed layout

The suggested antenna model's development and architecture are depicted in Figure 2(e)–(f). The designed antenna is etched on a low-cost FR4 epoxy thick substrate material with a relative dielectric permittivity of ε_r = 4.4, a loss tangent value of δ = 0.02, and a copper thickness of 0.035 mm. The suggested antenna is 28 mm long, 22 mm wide, and 1.5 mm thick. The intended antenna was created by modifying the metallic ground plane (MGP) and creating a small rectangular patch. On the top side of the laminate, a basic rectangular patch with compact dimensions of (10.5 × 14.0 mm^2) and a 50 **Ω** microstrip feed structure are etched, and a small miniature partial ground plane (PGP) is etched on the flip side of the substrate, as shown in Figure 2(a).

The chamfered operation of 5.0 mm is performed on the upper left and right edges of the PGP and constructs the antenna model-2 as shown in Figure 2(b). Further, an 8.0 mm fillet operation is performed on lower left and right edge of chamfered PGP to form an umbrella-shaped metallic ground plane (UsMGP), as depicted in Figure 2(c). The purpose of making this change on the PGP is to realize the high-performance features of the antenna. Then, as illustrated in Figure 2(d), trim the upper-right edge of the compact rectangular patch using a 3.0 mm fillet operation to create the antenna model-4.

Finally, the proposed antenna model is constructed by again applying fillet operation of 3.0 mm on the lower-left edge of rectangular patch and the loaded circular disc stub with the minimum size of 1.5 mm on the upper-right edge of the compact improved rectangular patch as elucidated in Figure 2(e). The variables and their optimal values of the proposed antenna design are listed in Table 1. The electromagnetic high frequency structure simulator (HFSS) software program develops and simulates the proposed antenna. Moreover, the proposed antenna model is also designed on the three dimensional (3D) altium designer (AD) tool widely used in the industry, as shown in Figure 2(f).

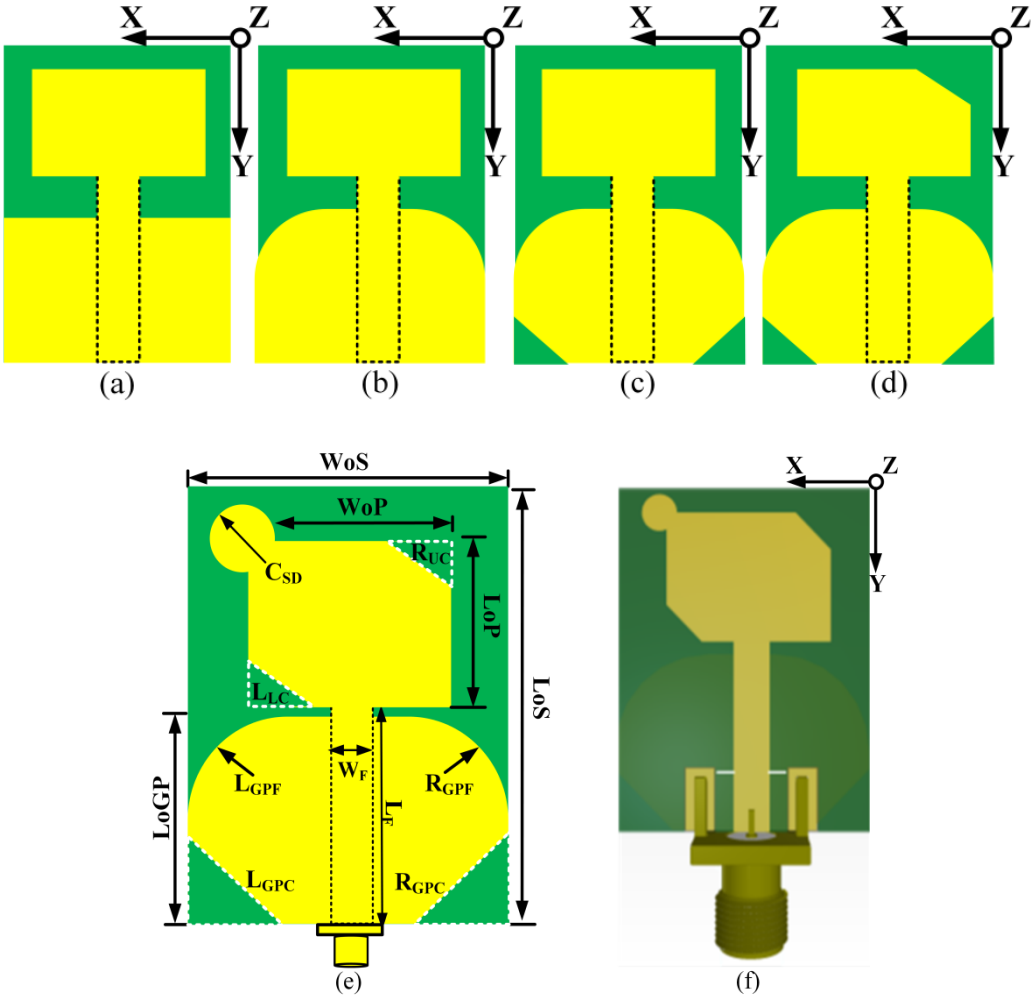

Figure 2. Proposed antenna development process, (a) simple partial ground plane (PGP), (b) chamfered PGP, (c) umbrella-shaped metallic ground plane (UsMGP), (d) fillet radiator and UsMGP, (e) proposed antenna prototype, (f) 3D designed antenna model with SMA connector.

Table 1. Proposed antenna designed variables and optimized values (unit: mm).

Defined variables	Optimized value	Defined Variables	Optimized value
WoS = WoGP	22.0	LoS	28.0
HoS	1.5	LoGP	14.5
$L_{GPC} = R_{GPC}$	8.0	$L_{GPF} = R_{GPF}$	5.0
W_F	3.1	L_F	17.0
LoP	14.0	WoP	10.5
$R_{UC} = L_{LC}$	3.0		C_{SD}1.5

The performance of the evolved antenna models in terms of return loss ($|S_{11}|$) is depicted in Figure 3; it is discovered that the initially designed antenna model obtained a wide impedance bandwidth (BW) of 4.9 GHz with a range of 3.9–8.8 GHz at a return loss of 10 dB. Additionally, the antenna model-2 has an impedance BW of 5.98 GHz and a frequency range of 3.78–9.76 GHz. The impedance BW is improved by 22% compared to the proposed antenna model-1. The partial ground

plane (PGP) is used to achieve this increase in impedance BW. Likewise, the antenna model-3 is designed to have an impedance BW of 6.08 GHz and a frequency range of 3.72–9.8 GHz. Moreover, the suggested antenna type achieves a greater impedance BW of 6.19 GHz over the 3.76–9.95 GHz frequency range. Finally, the proposed antenna model obtains an impedance BW of 7.76 GHz with a 3.65–11.41 GHz frequency range. Also, it can be seen that the proposed antenna model's impedance BW has been enhanced by 58.4% when compared to the initial antenna design model.

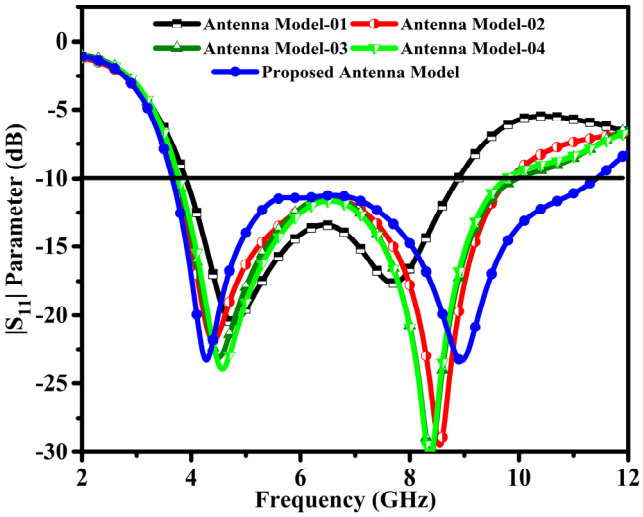

Figure 3. $|S_{11}|$ performance of overall antenna designed prototypes across the operable frequency.

4. Simulation results and discussion

This section explains the parametric analysis of the variables used to develop the proposed antenna design. The parameters associated with the intended variables can be examined by employing the electromagnetic high frequency structure simulator (HFSS) software package for rigorous multiple times simulation. The main purpose of this study is to obtain proper impedance matching, wide impedance BW and best performance results for the proposed antenna.

4.1. Influence of LoGP and WoP

The size of the length of the ground plane (LoGP) and width of the patch (WoP) influences the proposed antenna impedance matching performance and resonance tuning features. As shown in Figure 4(a), the proper impedance matching and wider BW are achieved at a maximum 14.5 mm value of the ground plane. Likewise, the second resonance tunability has been achieved at the maximum value of the variable. Further, the proper matching, wider impedance BW and second resonance tuning are achieved at the value of WoP 14.0 mm, as shown in Figure 4(b).

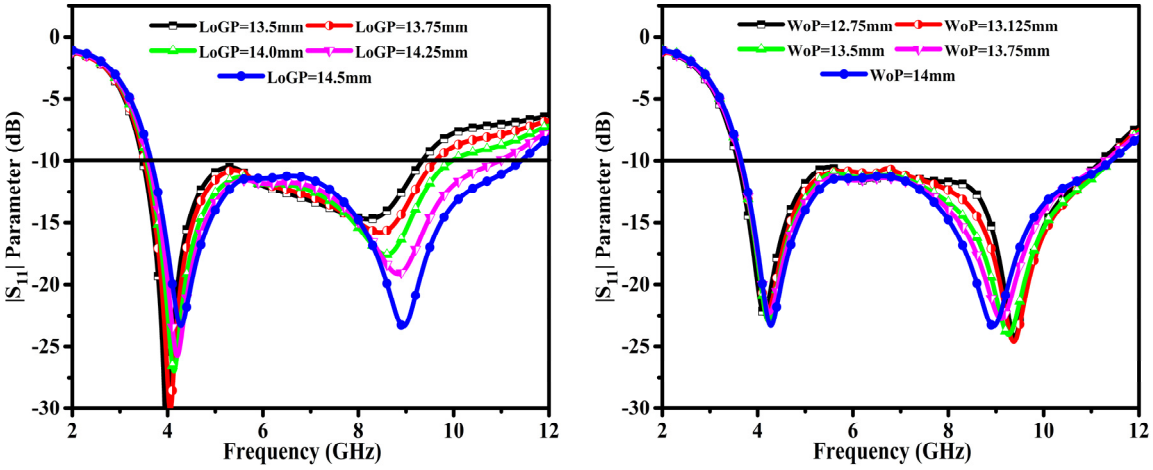

(**a**) (**b**)

Figure 4. Influence of variables over the entire operable frequency range, (a) length of ground plane LoGP, (b) width of the patch (WoP).

4.2. Influence of LoP and HoS

The length of the patch (LoP) and the thickness of the substrate (HoS) strongly influence the impedance matching, BW and frequency tuning performance of the proposed antenna. It can be analyzed from Figure 5(a); the antenna matching performance is achieved at the patch value of 10.5 mm. Further, substrate thickness strongly affects the impedance matching performance of the proposed antenna, as shown in Figure 5(b). It can be seen that at the lower value of the thickness of the substrate, the antenna exhibited the dual-band frequency response. The wider impedance BW is achieved at the optimized substrate thickness value of 1.5 mm.

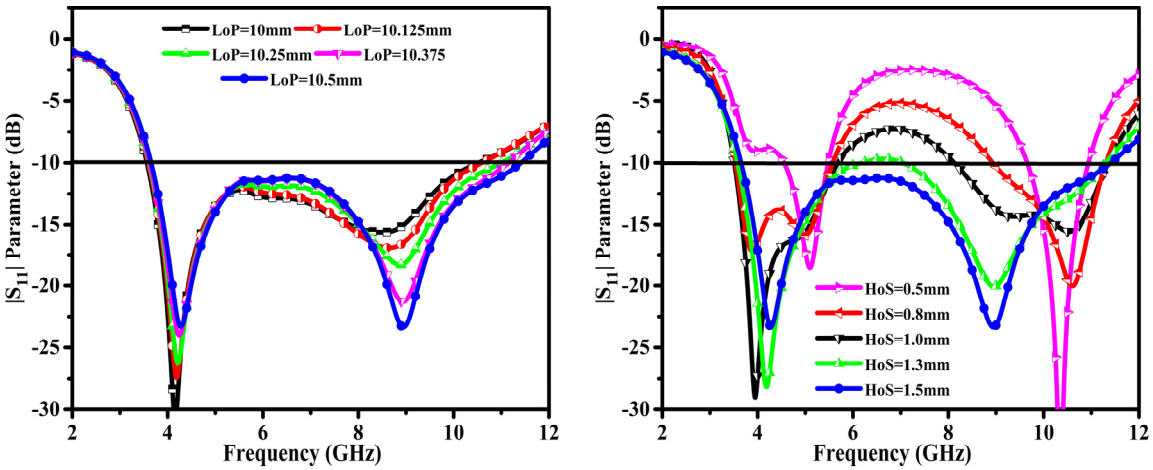

(**a**) (**b**)

Figure 5. Influence of parameters, (a) length of the patch (LoP) and (b) substrate thickness (HoS) across the operable frequency span.

4.3. Surface current distribution (J_{SURF})

The recommended antenna model's simulated result analysis of the current density at two resonances is presented in Figure 6(a)–(b). When the proposed antenna resonates at 4.82 GHz, it exhibits a significant distribution current across the entire patch, feeding line, and umbrella-shaped ground plane (UsMGP). Additionally, at 8.96 GHz, a slight shift in current is evaluated at the patch's upper edge and the UsMGP's lower left and right edges. As a result of the data stated previously, it can be inferred that the suggested antenna maneuvers admirably throughout the operable frequency range.

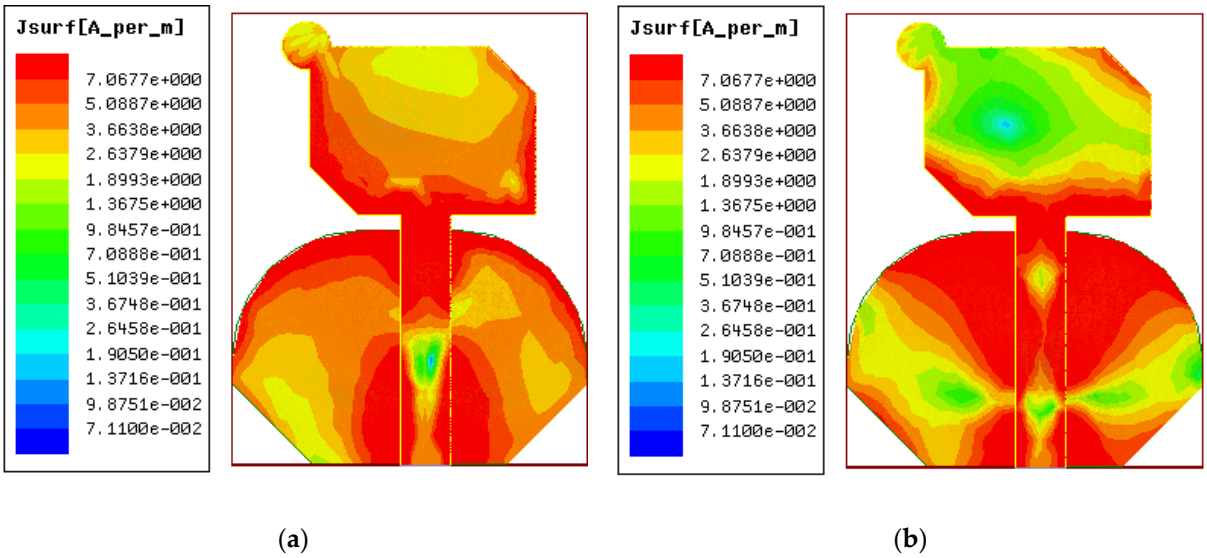

(**a**) (**b**)

Figure 6. Surface current distribution of the proposed antenna at different frequencies, (a) 4.28 GHz, (b) 8.96 GHz.

5. Experimental verified results

This section discusses the proposed antenna model's experimentally validated outcomes. The measured and simulated values for critical antenna characteristics such as $|S_{11}|$ (dB), peak realized gain (dBi), radiation efficiency (%), and radiation patterns throughout the standard plane are compared, investigated, and analyzed.

5.1. Return loss $|S_{11}|$ parameter

The manufactured antenna prototype is depicted in Figure 7(a)–(b). Before evaluating the return loss of the manufactured antenna sample, the vector network analyzer (VNA) is calibrated properly. The antenna model is linked to the VNA's single port. Figure 8 illustrates the simulation and measurement results for the proposed and manufactured antenna. The manufactured antenna sample's return loss ($|S_{11}|$) parameter performance is determined using the Agilent PNA 5230C VNA. As illustrated in Figure 8, the antenna's simulation model has a broader impedance bandwidth (BW) of 7.76 GHz, with a lower frequency of 3.65 GHz and a higher frequency of 11.41 GHz. Similarly, at 4.28 GHz and 8.96 GHz, two resonances are recorded. Additionally, the antenna's constructed model exhibits two resonances identical to the simulation model. As can be seen, the lower resonance has

been somewhat pushed away from 3.9 GHz compared to the simulation results. Due to the SMA connector's faulty welding and the lossy substrate material, discrepancies in the results have been noted.

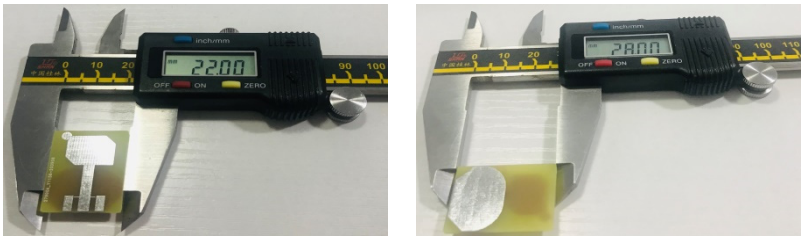

(**a**) (**b**)

Figure 7. Fabricated antenna model, (a) front view, (b) back view.

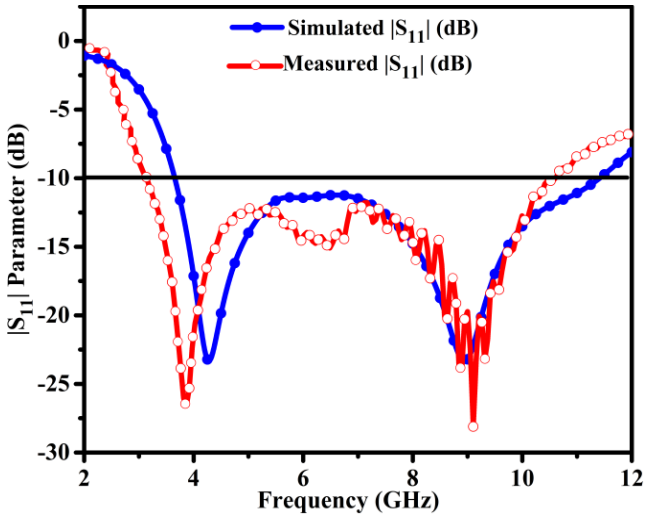

Figure 8. Simulation and measured results of $|S_{11}|$ entire operable frequency span.

5.2. Peak realized gain and Radiation efficiency

Figure 9(a) illustrates the simulation and measurement findings for the proposed antenna's peak realized gain. At 10.5 GHz, the planned antenna model's simulation result (streaked blue line) demonstrates a maximum gain of 4.58 dBi. Similarly, a respectable gain is noticed, for example, 4.13 dBi at 4.28 GHz and 4.42 dBi at 8.96 GHz resonances.

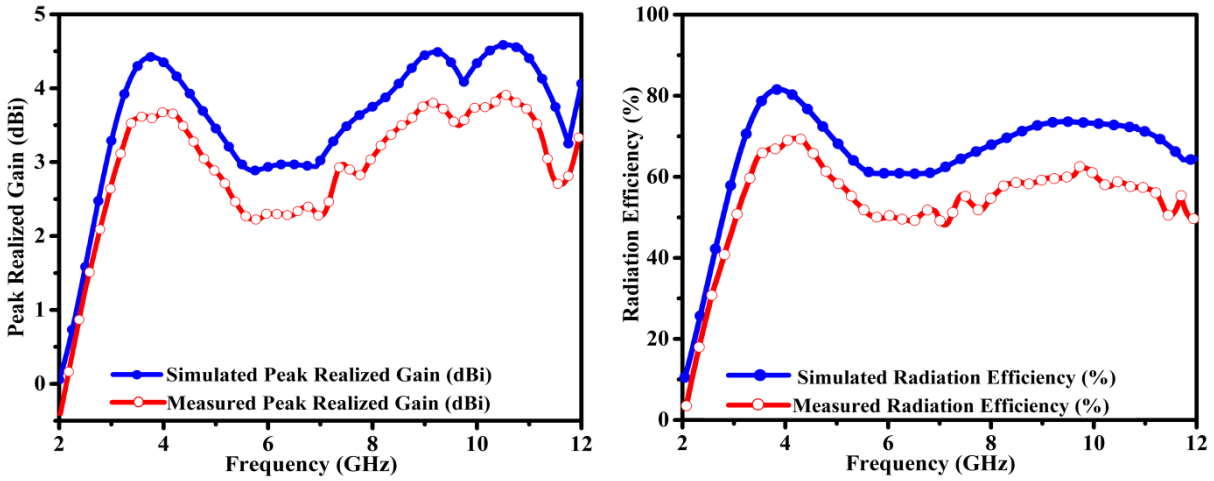

(**a**) (**b**)

Figure 9: Simulation and measurement results in the entire operating frequency range, (a) peak realized gain, (b) radiation efficiency.

Additionally, the Friis transmission equation is used to determine the measurement gain of the fabricated antenna. As illustrated in Figure 9(a), the manufactured sample of the antenna reaches a peak realized gain of 4.0 dBi at 10.5 GHz. Similarly, gain values of 3.7 dBi and 3.9 dBi are achievable at 4.28 GHz and 8.96 GHz resonances. Due to the loss of samples of the indoor antenna in the anechoic chamber during the measurement process, a difference of 0.58 dBi in the peak realized gain between the simulation and measurement data is seen.

Figure 9(b) depicts the proposed antenna's simulated and measured radiation efficiency. As can be seen, the antenna's maximum efficiency at 3.9 GHz is 82%. Similarly, the proposed antenna achieved a 78% and 70% radiation efficiency for 4.28 GHz and 8.96 GHz resonances. As can be seen, the suggested antenna radiates efficiently within the specified frequency range. Moreover, an efficient gain/directivity approach extracted the proposed fabricated antenna radiation efficiency. As illustrated in Figure 9(b) (streaked red line), the suggested antenna's fabricated sample reached a maximum efficiency of 72% at 4.5 GHz. Similarly, for resonant frequencies of 4.28 GHz and 8.96 GHz, the manufactured antenna sample approaches 70% and 60% radiation efficiency, respectively. Further, the difference observed in the simulation and measurement result of radiation efficiency is less than 20%, which validates the effectiveness of the applied gain directivity approach.

5.3. Radiation pattern performance

The manufactured antenna sample is put in an anechoic chamber to evaluate and validate the suggested antenna model's radiation pattern performance. The produced sample and ridge gap horn antenna are positioned in the line of sight (LoS), as seen in Figure 10(a)–(b). The fabricated antenna sample (the antenna under test) is mounted on the turntable and spun 360º.

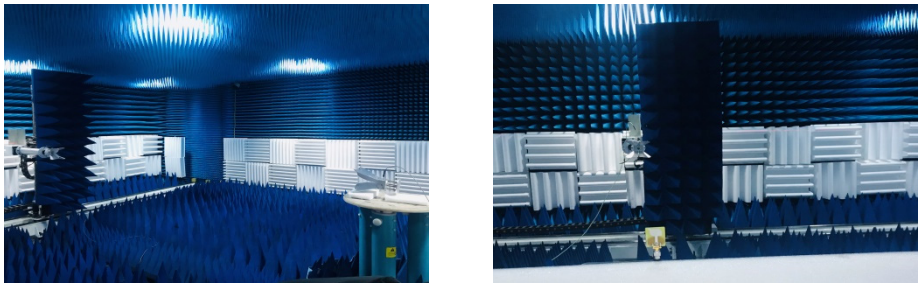

(**a**) (**b**)

Figure 10. Test environment of anechoic chamber room, (a) placement of ridge horn antennas, (b) placement of antenna under test (AUT).

The radiation pattern performance of the designed and fabricated model of an antenna on the standard planes (E-plane at Φ = 0º) and (H-plane at Φ = 90º) is shown in Figure 11(a)–(b). The proposed antenna model has excellent performance and presents the monopole-like radiation pattern on standard planes at the resonant frequency of 4.28 GHz, as elucidated in Figure 11(a). The simulation and measurement results are found to be consistent. Similarly, in the H-plane, nulls near 90º are formed.

Additionally, Figure 11(b) illustrates the suggested antenna's radiation pattern performance across standard planes at the resonant frequency of 8.96 GHz. The suggested antenna produces monopole-like radiation patterns along standard planes. Further, a zero point is established about 300º in the proposed antenna's H-plane. As a result of the preceding discussion, it can be concluded that the simulation results agree well with the measurement data. Similarly, for the resonant frequencies of 4.28 GHz and 8.96 GHz, the suggested antenna exhibits stable monopole-like radiation patterns along the standard planes.

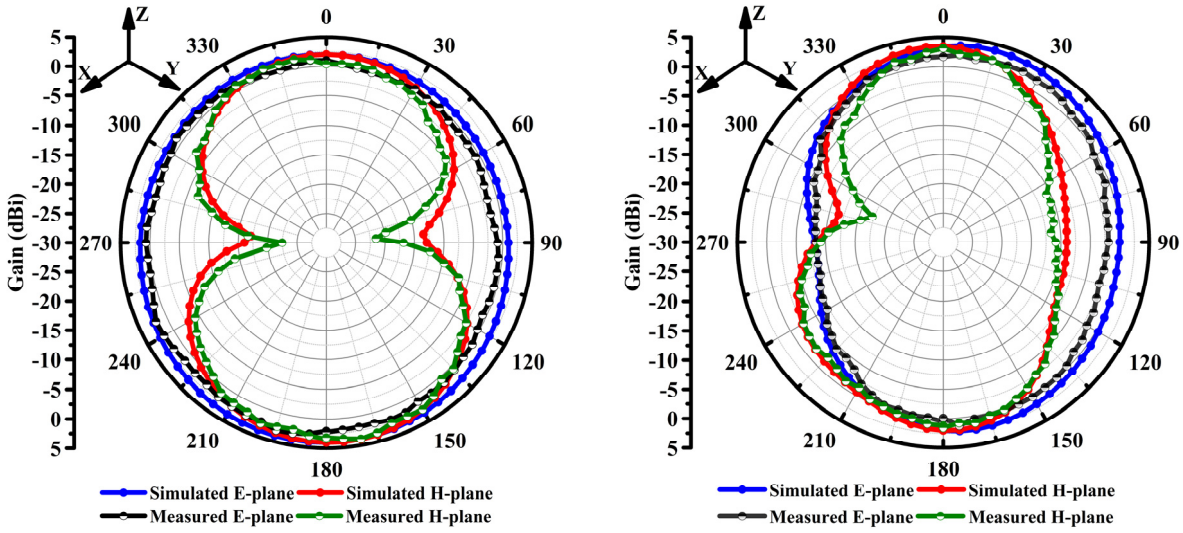

(**a**) (**b**)

Figure 11. The proposed antenna's simulation and measurement radiation patterns performance, (a) @4.28 GHz, (b) @8.96 GHz, on standard planes.

6. Performance comparison analysis

This section summarizes the suggested antenna's performance study regarding total occupied space, impedance bandwidth (BW), peak realized gain and radiation efficiency compared to previously published literature. As shown in Table 2, the proposed antenna achieved high gain values of 2.08 dBi, 1.08 dBi, and 0.58 dBi in comparison to the references [10,20,32]. The proposed antenna exhibits the higher impedance BW of 2.74 GHz, 4.54 GHz, 3.96 GHz and 4.16 GHz in comparison to the results reported in [10,13,19,32,53].

Further, the proposed antenna size is reduced by 34.18%, 70.8%, 86.96%, 90.98%, 74.26%, 90.94%, 41.3%, 70.83%, 85.4% and 99.69% as compared to investigated antennas in [18–21,27,28,39,40,61,62]. Furthermore, it is noted that the antenna radiation efficiency results in [19,21,27,28,61,62] are not reported. As shown in Table 2 and the above explained analysis, the proposed antenna is small in size and achieves a high performance compared to most recently examined antennas described in the literature.

Table 2. Performance comparison analysis of the proposed antenna with recently reported works.

Ref. / Year	Occupied space (mm^2)	Bandwidth (GHz)	Peak gain (dBi)	Efficiency (%)
This work / 2022	616	7.76	4.58	82
[27] / 2021	936	5.02	9.3	Not reported (NR)
[28] / 2020	2116	8.3	2.5	NR
[18] / 2019	4725	3.22	3.5	90
[19] / 2019	6832	8.01	6.5	NR
[20] / 2019	2393.6	8.9	7.0	90
[21] / 2018	6804	3.8	7.35	NR
[39] / 2018	1050	10	5.0	84
[40] / 2016	2112	3.6	4.0	95
[61] / 2016	4224	7.03	11.8	NR
[62] / 2015	202500	9.8	10	NR

7. Conclusions

In this article a novel compact broadband and radiation efficient antenna for medical IoT healthcare system has been proposed. The antenna design comprises of a compact improved radiator, umbrella-shaped metal ground plane (UsMGP) and 50 Ω microstrip feed line. In this research, a new hybrid technique is proposed to acquire the ideal antenna findings. The proposed approach is mainly based on etched slots and short load stubs employed on a partial ground plane (PGP) and rectangular patch. The suggested antenna is imprinted on a thick substrate made of a low-cost flame retardant material (FR4). The antenna has a compact dimension of 22 × 28 × 1.5 mm^3. The proposed antenna was carefully designed by using mathematical formulations extratcetd from the transmission line model. The parameters study of important variables involved in antenna design and its influence on impedance matching performance are analyzed. The designed antenna shows high performance, including 103% wide relative bandwidth, 82% best radiation efficiency, reasonable peak realized gain performance of 4.58 dBi, stable monopole-like radiation pattern and strong current distribution across the operable frequency span. The proposed antenna has been fabricated, and the experimental results have been validtated through simulation experiments. The designed antenna is suitable for M-IoT healthcare systems and covers heterogeneous wireless communication applications (HWCA).

Moreover, The presented work can be extended further to design, simulation and fabrication of the metamaterial inspired reconfigurable notch band MIMO antenna.

Acknowledgments

This research work is supported by the university research innovation fund of science and technology development center of the Ministry of education of China (2020ITA05022), the Natural Science Foundation of Hubei Province (2021CFB316), the Preliminary support project of Hubei Social Science Foundation (21ZD137), the Hundreds of Schools Unite with Hundreds of Counties-University Serving Rural Revitalization Science and Technology Support Action Plan (BXLBX0847). Further, the authors greatly acknowledge the technical and industrial support provided by the Nanjing Hurys Intelligent Technology Company Limited and the experimental facility in measuring the fabricated antenna model at the Nanjing University of Aeronautics and Astronautics (NUAA) China.

Conflict of interest

The authors declare that there is no conflict of interest regarding the publication of this manuscript.

References

1. M. S. Islam, M. T. Islam, M. A. Ullah, G. K. Beng, N. Amin, N. Misran, A modified meander line microstrip patch antenna with enhanced bandwidth for 2.4 GHz ISM-band internet of things (IoT) applications, *IEEE Access*, **7** (2019), 127850–127861. https://doi.org/10.1109/ACCESS.2019.2940049
2. M. Bansal, B. Gandhi, IoT based development boards for smart healthcare applications, in *2018 4th International Conference on Computer Communication Automation (ICCCA)*, (2018), 1–7. https://doi.org/10.1109/CCAA.2018.8777572
3. K. R. Jha, B. Bukhari, C. Singh, G. Mishra, S. K. Sharma, Compact planar multistandard MIMO antenna for IoT applications, *IEEE Trans. Antennas Propag.*, **66** (2018), 3327–3336. https://doi.org/10.1109/TAP.2018.2829533
4. B. J. Falkner, H. Zhou, A. Mehta, T. Arampatzis, D. Mirshekar-syahkal, H. Nakano, A circularly polarized low-cost flat panel antenna array with a high impedance surface meta-substrate for satellite on-the-move medical IoT applications, *IEEE Trans. Antennas Propag.* **69** (2021), 6076–6081. https://doi.org/10.1109/TAP.2021.3070011
5. B. Pradhan, S. Bhattacharyya, K. Pal, IoT-based applications in healthcare devices, *J. Healthcare Eng.*, **2021** (2021). https://doi.org/10.1155/2021/6632599
6. T. Han, L. Zhang, S. Pirbhulal, W. Wu, V. H. C. de Albuquerque, A novel cluster head selection technique for edge-computing based IoMT systems, *Comput. Networks*, **158** (2019), 114–122. https://doi.org/10.1016/j.comnet.2019.04.021
7. S. Pirbhulal, H. Zhang, Md. E. E. Elahi, H. Ghavyat, S. C. Mukhopadhyay, Y. T. Zhang, et al., A novel secure IoT-based smart home automation system using a wireless sensor network, *Sensors (Switzerland)*, **17** (2017), 1–19. https://doi.org/10.3390/s17010069

8. M. Pazhoohesh, M. S. Javadi, M. Gheisari, S. Aziz, R. Villa, Dealing with missing data in the smart buildings using innovative imputation techniques, in *IECON 2021–47th Annual Conference of the IEEE Industrial Electronics Society*, (2021), 1–7, https://doi.org/10.1109/iecon48115.2021.9612650
9. A. H. Sodhro, S. Pirbhulal, M. Qaraqe, S, Lohano, G. H. Sodhro, N. R. Junejo, et al., Power control algorithms for media transmission in remote healthcare systems, *IEEE Access*, **6** (2018), 42384–42393. https://doi.org/10.1109/ACCESS.2018.2859205
10. S. Pirbhulal, H. Zhang, S. C. Mukhopadhyay, C. Li, Y. Wang, G. Li, et al., An efficient biometric-based algorithm using heart rate variability for securing body sensor networks, *Sensors (Switzerland)*, **15** (2015), 15067–15089. https://doi.org/10.3390/s150715067
11. Y. Guan, M. Aamir, Z. Rahman, A. Ali, W. A. Abro, Z. A. Dayo, et al., A framework for efficient brain tumor classification using MRI images, *Math. Biosci. Eng.*, **18** (2021), 5790–5815. https://doi.org/10.3934/MBE.2021292
12. A. H. Sodhro, S. Pirbhulal, A. K. Sangaiah, S. Lohano, G. H. Sodhro, Z. Luo, 5G-based transmission power control mechanism in fog computing for internet of things devices, *Sustainability*, **10** (2018), 1–17. https://doi.org/10.3390/su10041258
13. S. B. Baker, W. Xiang, I. Atkinson, Internet of things (IoT) for smart healthcare: technologies, challenges and opportunities, *IEEE Access*, **5** (2017), 26521–26544. https://doi.org/10.1109/ACCESS.2017.2775180
14. S. Pirbhulal, H. Zhang, W. Wu, S. C. Mukhopadhyay, Y. T. Zhang, Heartbeats based biometric random binary sequences generation to secure wireless body sensor networks, *IEEE Trans. Biomed. Eng.*, **65** (2018), 2751–2759. https://doi.org/10.1109/TBME.2018.2815155
15. Z. A. Dayo, Q. Cao, Y. Wang, S. Pirbhulal, A. H. Sodhro, A compact high-gain coplanar waveguide-fed antenna for military RADAR applications, *Int. J. Antennas Propag.*, **2020** (2020), 1–10. https://doi.org/10.1155/2020/8024101
16. T. Gayatri, N. Anveshkumar, V. K. Sharma, A compact planar UWB antenna for spectrum sensing in cognitive radio, in *International Conference on Emerging Trends in Information Technology and Engineering*, (2020), 1–5. https://doi.org/10.1109/ic-ETITE47903.2020.384
17. P. Soothar, H. Wang, C. Xu, Z. A. Dayo, B. Muneer, K. Kanwar, A compact broadband and high gain tapered slot antenna with stripline feeding network for H, X, Ku and K band applications, *Int. J. Adv. Comput. Sci. Appl.*, **11** (2020), 239–244. https://doi.org/10.14569/IJACSA.2020.0110731
18. S. Das, H. Islam, T. Bose, N. Gupta, Ultra wide band CPW-fed circularly polarized microstrip antenna for wearable applications, *Wirel. Pers. Commun.*, **108** (2019), 87–106. https://doi.org/10.1007/s11277-019-06389-9
19. G. Bozdag, M. Secmen, Compact wideband tapered-fed printed bow-tie antenna with rectangular edge extension, *Microw. Opt. Technol. Lett.*, **61** (2019), 1394–1399. https://doi.org/10.1002/mop.31733
20. L. Guo, M. Min, W. Che, W. Yang, A novel miniaturized planar ultra-wideband antenna, *IEEE Access*, **7** (2019), 2769–2773. https://doi.org/10.1109/ACCESS.2018.2886799
21. M. Li, Y. Zhang, M. C. Tang, Design of a compact, wideband, bidirectional antenna using index-gradient patches, *IEEE Antennas Wirel. Propag. Lett.*, **17** (2018), 1218–1222. https://doi.org/10.1109/LAWP.2018.2839900

22. Y. H. Lee, E. H. Lim, F. L. Bong, B. K. Chung, Compact folded C-shaped antenna for metal-mountable UHF RFID applications, *IEEE Trans. Antennas Propag.*, **67** (2019), 765–773. https://doi.org/10.1109/TAP.2018.2879853
23. N. Jaglan, S. D. Gupta, B. K. Kanaujia, S. Srivastava, Band notched UWB circular monopole antenna with inductance enhanced modified mushroom EBG structures, *Wirel. Networks*, **24** (2018), 383–393. https://doi.org/10.1007/s11276-016-1343-7
24. P. K. Jain, B. R. Sharma, K. G. Jangid, S. Shekhawat, V. K. Saxena, D. Bhatnagar, Elliptical shaped wide slot monopole patch antenna with crossed shaped parasitic element for WLAN, Wi-MAX, and UWB application, *Microw. Opt. Technol. Lett.*, **62** (2020), 899–905. https://doi.org/10.1002/mop.32100
25. S. Baudha, M. V. Yadav, A novel design of a planar antenna with modified patch and defective ground plane for ultra-wideband applications, *Microw. Opt. Technol. Lett.*, **61** (2019), 1320–1327. https://doi.org/10.1002/mop.31716
26. Y. Zhao, C. Wang, Y. Deng, C. Xie, A novel compact ultra-wideband antenna with quad notched bands based on s-sCRLHs resonator, *Wirel. Pers. Commun.*, **97** (2017), 4667–4679. https://doi.org/10.1007/s11277-017-4744-8
27. N. Gupta, J. Saxena, K. S. Bhatia, R. Kumar, A compact CPW-fed planar stacked circle patch antenna for wideband applications, *Wirel. Pers. Commun.*, **116** (2021), 3247–3260. https://doi.org/10.1007/s11277-020-07847-5
28. A. Joshi and R. Singhal, Probe-Fed Hexagonal Ultra Wideband Antenna Using Flangeless SMA Connector, *Wireless Pers. Commun.*, **110** (2020), 973–982. https://doi.org/10.1007/s11277-019-06768-2
29. K. P. Ray, S. S. Thakur, Modified trident UWB printed monopole antenna, *Wirel. Pers. Commun.*, **109** (2019), 1689–1697. https://doi.org/10.1007/s11277-019-06646-x
30. S. Y. A. Fatah, E. K. Hamad, W. Swelam, A. Allam, M. F. A. Sree, H. A. Mohamed, Design and implementation of UWB slot-loaded printed antenna for microwave and millimeter wave applications, *IEEE Access*, **9** (2021), 29555–29564. https://doi.org/10.1109/ACCESS.2021.3057941
31. Q. Y. Guo, H. Wong, Wideband and high-gain fabry–pérot cavity antenna with switched beams for milimeter-wave applications, **67** (2019), 4339–4347. https://doi.org/10.1109/TAP.2019.2905781
32. R. V. Gatti, R. Rossi, M. Dionigi, Single-layer line-fed broadband microstrip patch antenna on thin substrates, *Electronics (Switzerland)*, **10** (2021), 1–14. https://doi.org/10.3390/electronics10010037
33. M. V. Yadav, S. Baudha, A miniaturized printed antenna with extended circular patch and partial ground plane for UWB applications, *Wirel. Pers. Commun.*, **116** (2021), 311–323. doi: https://doi.org/10.1007/s11277-020-07716-1
34. K. P. Ray, Design aspects of printed monopole antennas for ultra-wide band applications, *Int. J. Antennas Propag.*, **2008** (2008), 1–8. https://doi.org/10.1155/2008/713858
35. S. Baudha, V. D.Kumar, Miniaturized dual broadband printed slot antenna with parasitic slot and patch, *Microw. Opt. Technol. Lett.*, **56** (2014), 2260–2265. https://doi.org/10.1002/mop.28567
36. H. Fallahi, Z. Atlasbaf, Bandwidth enhancement of a cpw-fed monopole antenna with small fractal elements, *AEU Int. J. Electron. Commun.*, **69** (2015), 590–595. doi: https://doi.org/10.1016/j.aeue.2014.11.011

37. Y. Z. Cai, H. C. Yang, L. Y. Cai, Wideband monopole antenna with three band-notched characteristics, *IEEE Antennas Wirel. Propag. Lett.*, **13** (2014), 607–610. doi: https://doi.org/10.1109/LAWP.2014.2313178
38. C. Kumar, D. Guha, Higher mode discrimination in a rectangular patch: new insight leading to improved design with consistently low cross-polar radiations, *IEEE Trans. Antennas Propag.*, **69** (2021), 708–714. https://doi.org/10.1109/TAP.2020.3016506
39. S. Kundu, S. K. Jana, A compact umbrella shaped UWB antenna for ground-coupling GPR applications, *Microw. Opt. Technol. Lett.*, **60** (2018), 146–151. https://doi.org/10.1002/mop.30928
40. H. T. Hu, F. C. Chen, Q. X. Chu, A wideband u-shaped slot antenna and its application in MIMO terminals, *IEEE Antennas Wirel. Propag. Lett.*, **15** (2016), 508–511. https://doi.org/10.1109/LAWP.2015.2455237
41. S. K. Palaniswamy, K. Malathi, A. K. Shrivastav, Palm tree structured wide band monopole antenna, *Int. J. Microw. Wirel. Technol.*, **8** (2016), 1077–1084. https://doi.org/10.1017/S1759078715000434
42. M. Sharma, Y. K. Awasthi, H. Singh, Design of compact planar triple band-notch monopole antenna for ultra-wideband applications, *Wirel. Pers. Commun.*, **97** (2017), 3531–3545. https://doi.org/10.1007/s11277-017-4684-3
43. P. Kumar, A. Chaturvedi, Design and development of single & dual resonant frequency antennas for moisture content measurement, *Wirel. Pers. Commun.*, **114** (2020), 565–582. https://doi.org/10.1007/s11277-020-07382-3
44. P. V. Naidu, A. Malhotra, A small ACS-fed tri-band antenna employing C and L shaped radiating branches for LTE/WLAN/WiMAX/ITU wireless communication applications, *Analog Integr. Circuits Signal Process.*, **85** (2015), 489–496. https://doi.org/10.1007/s10470-015-0637-5
45. Z. A. Dayo, Q. Cao, P. Soothar, M. M. Lodro, Y. Li, A compact coplanar waveguide feed bow-tie slot antenna for WIMAX, C and X band applications, in *2019 IEEE International Conference on Computational Electromagnetics (ICCEM) Shanghai China*, (2019), 1–3, https://doi.org/10.1109/COMPEM.2019.8779099
46. Z. A. Dayo, Q. Cao, Y. Wang, P. Soothar, A compact high gain multiband bow-tie slot antenna, in *2019 International Applied Computational Electromagnetics Society Symposium-China (ACES)*, **1** (2019), 1–2. https://doi.org/10.23919/ACES48530.2019.9060736
47. M. A. Ullah, T. Alam, M. T. Islam, A UHF CPW-fed patch antenna for nanosatellite store and forward mission, *Microsyst. Technol.*, **26** (2020), 2399–2405. https://doi.org/10.1007/s00542-020-04780-2
48. S. Naser, N. Dib, Design and analysis of super-formula-based UWB monopole antenna and its MIMO configuration, *Wirel. Pers. Commun.*, **94** (2017), 3389–3401. https://doi.org/10.1007/s11277-016-3782-y
49. N. Prasad, G. Mithilesh, Development of a reconfigurable and miniaturized CPW antenna for selective and wideband communication, *Wirel. Pers. Commun.*, **95** (2017), 2599–2608. https://doi.org/10.1007/s11277-017-3942-8
50. L. Zhang, Y. Sun, Y. He, S. W. Wong, C. Mao, L. Gei, et al., A quad-polarization reconfigurable antenna with suppressed cross polarization based on characterstics mode theory, *IEEE Trans. Antennas Propag.*, **69** (2021), 636–647. https://doi.org/10.1109/TAP.2020.3016384

51. Z. A. Dayo, Q. Cao, Y. Wang, P. Soothar, I. A. Khoso, G. Shah, et al., A compact high gain multiband bowtie slot antenna with miniaturized triangular shaped metallic ground plane, *Appl. Comput. Electromagn. Soc. J.*, **36** (2021), 935–945. https://doi.org/10.47037/2021.ACES.J.360717
52. A. Kurniawan, S. Mukhlishin, Wideband antenna design and fabrication for modern wireless communications systems, in *Procedia Technology (Iceei)*, **11** (2013), 348–353. https://doi.org/10.1016/j.protcy.2013.12.201
53. Z. A. Dayo, Q. Cao, Y. Wang, P. Soothar, B. Muneer, B. S. Chowdhry, A compact broadband high gain antenna using slotted inverted omega shape ground plane and tuning stub loaded radiator, *Wirel. Pers. Commun.*, **113** (2020), 499–518. https://doi.org/10.1007/s11277-020-07227-z
54. K. E. Kedze, H. Wang, Y. Kim, I. Park, Design of a reduced-size crossed-dipole antenna, *IEEE Trans. Antennas Propag.*, **69** (2021), 689–697. https://doi.org/10.1109/TAP.2020.3016392
55. W. Mazhar, D. M. Klymyshyn, G. Wells, A. A. Qureshi, M. Jacobs, S. Achenbach, Low-profile artificial grid dielectric resonator antenna arrays for mm-wave applications, *IEEE Trans. Antennas Propag.*, **67** (2019), 4406–4417. https://doi.org/10.1109/TAP.2019.2907610
56. P. Soothar, H. Wang, B. Muneer, Z. A. Dayo, B. S. Chowdhry, A broadband high gain rapered slot antenna for underwater communication in microwave band, *Wirel. Pers. Commun.*, **116** (2021), 1025–1042. https://doi.org/10.1007/s11277-019-06633-2
57. L. Z. Song, P. Y. Qin, S. Maci, Y. J. Guo, Ultrawideband conformal transmitarray employing connected slot-bowtie elements, *IEEE Trans. Antennas Propag.*, **69** (2021), 3273–3283. https://doi.org/10.1109/TAP.2020.3037785
58. J. Wu, C. Wang, Y. X. Guo, A compact reflector antenna fed by a composite S/Ka-band feed for 5G wireless communications, *IEEE Trans. Antennas Propag.*, **68** (2020), 7813–7821. https://doi.org/10.1109/TAP.2020.3000858
59. S. Soltani, P. Lotfi, R. D. Murch, Design and optimization of multiport pixel antennas, *IEEE Trans. Antennas Propag.,* **66** (2018), 2049–2054. https://doi.org/10.1109/TAP.2018.2800759
60. Z. A. Dayo, Q. Cao, Y. Wang, S. U. Rahman, P. Soothar, A compact broadband antenna for civil and military wireless communication applications, *Int. J. Adv. Comput. Sci. Appl.*, **10** (2019), 39–44. https://doi.org/10.14569/ijacsa.2019.0100906
61. J. Y. Li, R. Xu, X. Zhang, S. G. Zhou, G. W. Yang, A wideband high-gain cavity-backed low-profile dipole antenna, *IEEE Trans. Antennas Propag.*, **64** (2016), 5465–5469. https://doi.org/10.1109/TAP.2016.2620607
62. T. H. Jung, S. C. Jung, H. K. Ryu, H. S. Oh, J. M. Woo, Ultrawideband planar dipole antenna with a modified taegeuk structure, *IEEE Antennas Wirel. Propag. Lett.*, **14** (2015), 194–197. https://doi.org/10.1109/LAWP.2014.2359936